

## Supporting Information

# Formation of core/corona nanoparticles with interpolyelectrolyte complex cores in aqueous solution: Insight in chain dynamics in the complex from fluorescence quenching

Anastasiia Murmiliuk<sup>a</sup>, Pavel Matějčíček<sup>a</sup>, Sergey K. Filippov<sup>b</sup>, Miroslav Janata<sup>b</sup>, Miroslav Šlouf<sup>b</sup>, Stergios Pispas<sup>c</sup> and Miroslav Štěpánek<sup>a</sup>

<sup>a</sup>*Department of Physical and Macromolecular Chemistry, Charles University, Hlavova 8, 128 00 Prague 2, Prague, Czech Republic, stepanek@natur.cuni.cz*

<sup>b</sup>*Institute of Macromolecular Chemistry, Czech Academy of Sciences, Heyrovský Square 2, 162 06 Prague 6, Czech Republic*

<sup>c</sup>*Theoretical and Physical Chemistry Institute, National Hellenic Research Foundation, 48 Vassileos Constantinou Avenue, 11635 Athens, Greece*

### Contents:

1. Synthesis and characterization of umbelliferone-labeled PMAA
2. Fitting SAXS curves of QNPHOS-PEO and QNPHOS-PEO/PMAA solutions
3. AFM scans of QNPHOS-PEO/PMAA aggregates on mica
4. Thermodynamics and kinetics of PMAA/QNPHOS-PEO complexation from ITC experiments
5. Fluorescence emission spectra and emission decays of umbelliferone in PMAA and QNPHOS-PEO/PMAA solutions
6. Transmittance spectrum of QNPHOS-PEO/PMAA solution

### 1. Synthesis and characterization of umbelliferone-labeled PMAA (Fig. S1)

*Materials.* 1,3-Dihydroxybenzene (resorcinol; 99%, Sigma-Aldrich), ethyl 4-chloroacetoacetate (95%, Sigma-Aldrich), sulphuric acid (95%, Lach-Ner, Czech Republic), copper(I) chloride (97%, Sigma-Aldrich), copper(II) chloride (97%, Sigma-Aldrich),

1,1,4,7,10,10-hexamethyltriethylenetetramine (HMTETA; 97%, Sigma-Aldrich), tetrahydrofuran (THF; Lach-Ner, Czech Republic), dichloromethane (Lach-Ner), trifluoroacetic acid (99.5%, Acros) were used as received. Toluene was distilled with lithium aluminum hydride. *Tert*-butyl methacrylate was distilled with calcium hydride and with triisobutyl aluminum before use.

*Characterization methods.* Size exclusion chromatography (SEC) of umbelliferone-labeled poly(*tert*-butyl methacrylate) precursor was performed at 25 °C with two PLgel MIXED-C columns (300 × 7.5 mm, SDV gel with particle size 5µm; Polymer Laboratories, USA) and with UV (UVD 250; Watrex, Czech Republic; detection wavelength 260 nm) and RI (RI-101; Shodex, Japan) detectors. Tetrahydrofuran was used as a mobile phase at a flow rate of 1 mL/min. The molecular weight values were calculated using Clarity software (Dataapex, Czech Republic). Calibration with poly(methyl methacrylate) standards (PSS, Germany) was used. <sup>1</sup>H NMR spectra of 4-chloromethylumbelliferone initiator and umbelliferone-labeled poly(methacrylic acid) were measured in dimethyl sulfoxide (DMSO-*d*<sub>6</sub>) at 22 °C using a Bruker DPX 300 spectrometer at 300.1 MHz. Hexamethyldisiloxane (HMDSO) was used as an internal standard.

*Synthesis of 4-chloromethylumbelliferone (4-chloromethyl-7-hydroxycoumarin) initiator.* Crushed 1,3-dihydroxybenzene (5.6 g, 50.86 mmol) was added portionwise with stirring to sulphuric acid (43 mL) in an ice-water bath. To the resulting suspension, ethyl 4-chloroacetoacetate (5.7 mL, 42.5 mmol) was added dropwise under cooling. The reaction mixture was intensively stirred for 2 h under cooling, subsequently for 24 h at room temperature, and then it was poured portionwise to ice-cold water (400 mL). The resulting mixture with ochreous precipitate was stirred for ca 1 h at room temperature, filtered and the solid product was washed with ice-cold water to neutral reaction. The isolated product was then recrystallized from ethanol and dried at 40 °C in vacuum. The yield was 6.7 g.

<sup>1</sup>H-NMR (DMSO, Fig. S2): 4.95 ppm (CH<sub>2</sub>Cl), 6.41–7.68 ppm (protons at carbons C3, C5, C6, and C8), 10.65 ppm (OH).

*ATRP polymerization of tert-butyl methacrylate initiated with 4-chloromethylumbelliferone.* Copper(I) chloride (8.46 mg, 0.085 mmol), copper(II) chloride (5.75 mg, 0.043 mmol), and 4-chloromethylumbelliferone (3.6 mg, 0.017 mmol) were placed in the reaction flask. After several vacuum/argon cycles toluene (4.2 mL), *tert*-butyl methacrylate (4.2 mL, 25.6 mmol) and HMTETA (0.023 mL, 0.085 mmol) were added sequentially. Polymerization was carried out at 90 °C for 24 h. Polymerization mixture was

then diluted with THF and precipitated in 70% methanol. Isolated polymer, umbelliferone-labeled poly(*tert*-butyl methacrylate), was dried at 40 °C in vacuum. The yield was 1.75 g.

SEC (THF, Fig. S3):  $M_n = 179\,000$ ,  $M_w/M_n = 1.14$ . The response from the UV detector (curve 2) clearly proved that the prepared poly(*tert*-butyl methacrylate) was labeled with the umbelliferone moiety.

*Transformation of umbelliferone-labeled poly(tert-butyl methacrylate) to umbelliferone-labeled poly(methacrylic acid).* Umbelliferone-labeled poly(*tert*-butyl methacrylate) (1.39 g) was placed in the reaction flask. After several vacuum/argon cycles dichloromethane (40 mL) and trifluoroacetic acid (3.6 mL) were added. The reaction solution was stirred at room temperature for 24 h. The reaction mixture was then evaporated to dryness, the solid product was solubilized in absolute ethanol and the solution was precipitated in hexane. Isolated product, umbelliferone-labeled poly(methacrylic acid), was dried at 40 °C in vacuum for 48 h. The yield was 0.88 g.

$^1\text{H-NMR}$  (DMSO, Fig. S4): 0.8–1.1 ppm ( $\alpha\text{-CH}_3$ ), 1.7 ppm (backbone  $\text{CH}_2$ ), 6–8 ppm (protons at carbons C3, C5, C6, and C8 of umbelliferone label), 10.5 ppm (OH proton of umbelliferone label), 12.3 ppm (COOH).

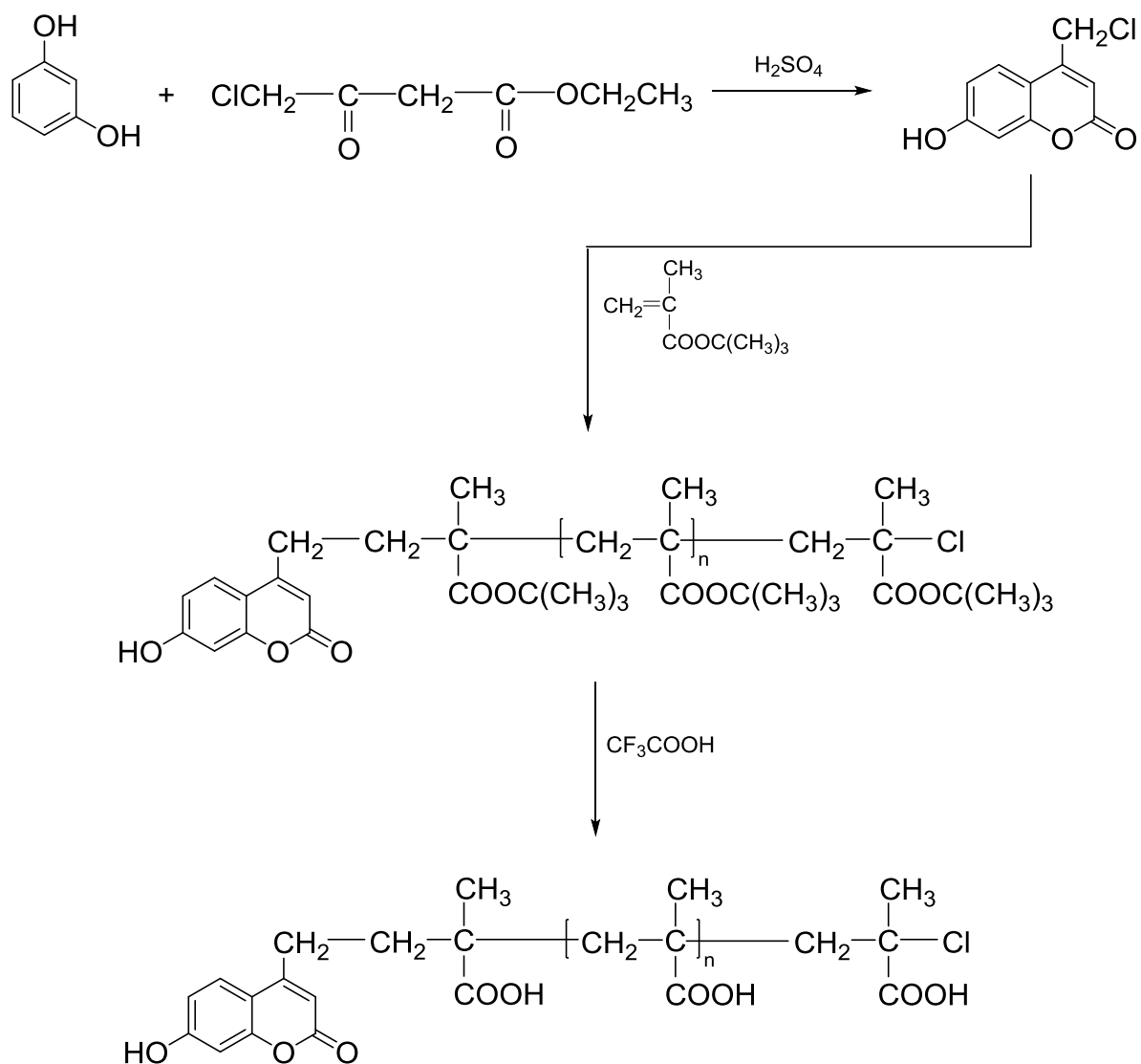


**Fig. S1.** Reaction scheme of the synthesis of umbelliferone-labeled PMAA.

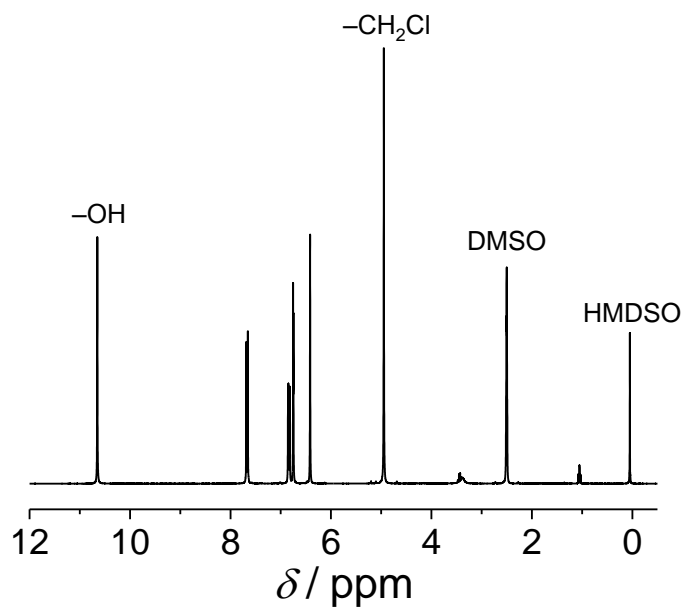


**Fig. S2.**  $^1\text{H}$  NMR spectrum of 4-chloroumbelliferone.

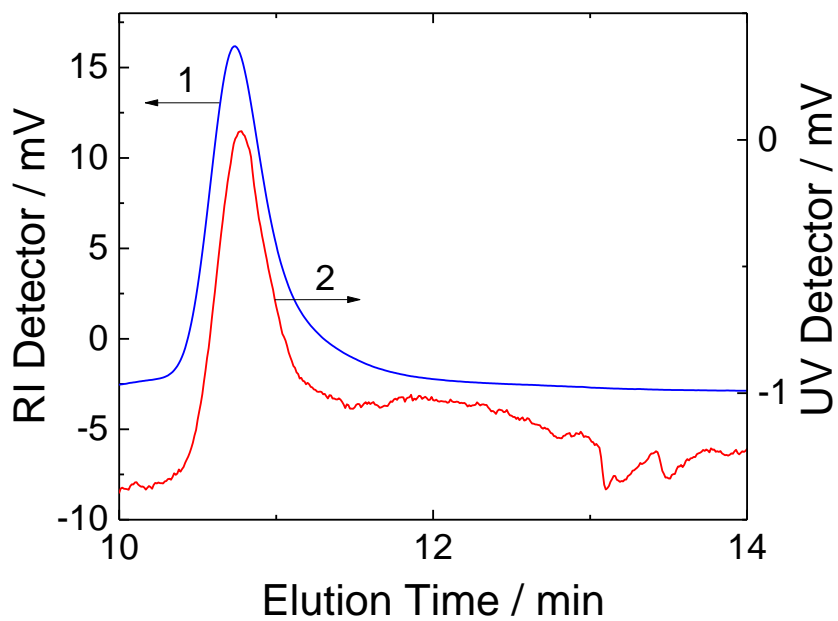


**Fig. S3.** SEC chromatogram of umbelliferone-labeled poly(*tert*-butyl methacrylate) with the refractive index detector (curve 1) and the UV detector operating at 260 nm (curve 2).

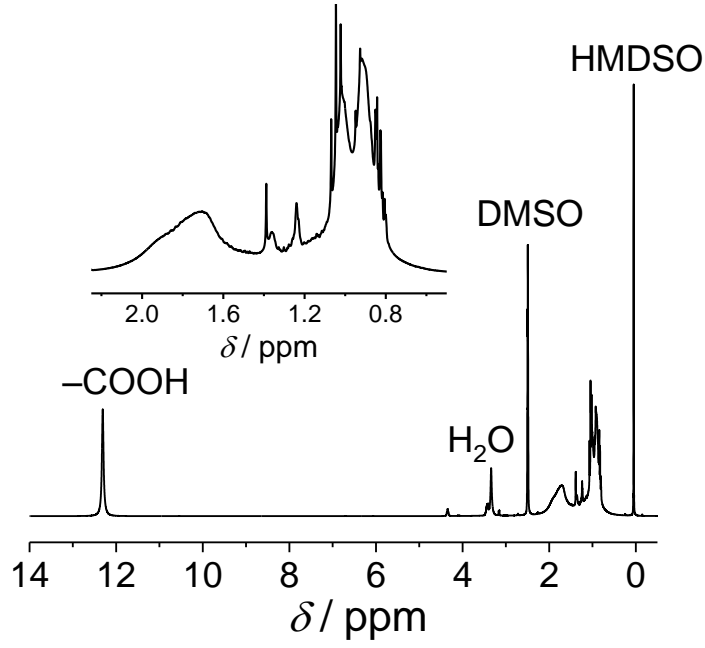


**Fig. S4.**  $^1\text{H}$  NMR spectrum of umbelliferone-labeled PMAA. Insert: Detail of the spectrum for 2.25–0.5 ppm.

## 2. Fitting SAXS curves of QNPHOS-PEO and QNPHOS-PEO/PMAA solutions

The SAXS curve from the QNPHOS-PEO solution was fitted to the model of the generalized Gaussian coil. Attractive interactions between the coils were treated by the mass fractal structure factor with the exponential cutoff for the pair correlation function:

$$I(I_0, q, R_g, \nu, D, \xi, r_0) = I_0 \left\{ 1 + \frac{D\Gamma(D-1) \sin[(D-1) \arctan(q\xi)]}{(qr_0)^D (1 + q^{-2}\xi^{-2})} \right\} \times \frac{U^{1/2\nu} \Gamma(\frac{1}{2\nu}) - \Gamma(\frac{1}{\nu}) - U^{1/2\nu} \Gamma(\frac{1}{2\nu}, U) + \Gamma(\frac{1}{\nu}, U)}{\nu U^{1/\nu}} \quad (\text{S1})$$

where  $I_0$  is the forward scattering,  $r_g$  is the gyration radius,  $\nu$  is the excluded volume parameter,  $D$  is the mass fractal dimension,  $\xi$  is the correlation length of the fractal cluster, and  $r_0$  is the characteristic dimension of a particle forming the cluster and the gamma function ( $\Gamma(a) = \Gamma(a, 0)$ ) and the parameter  $U$  are defined as

$$\Gamma(a, x) = \int_x^\infty t^{-a} \exp(-t) dt \quad (\text{S2})$$

$$U = (2\nu + 1)(2\nu + 2) \frac{R_g^2 q^2}{6} \quad (\text{S3})$$

The fit provided the values  $I_0 = 0.028 \pm 0.0009 \text{ cm}^{-1}$ ;  $R_g = 9.8 \pm 0.2 \text{ nm}$ ;  $\nu = 0.635 \pm 0.001$ ,  $\xi = 88 \pm 5 \text{ nm}$ ;  $D = 1.89 \pm 0.12 \text{ nm}$ ;  $r_0 = 32 \pm 1 \text{ nm}$ .

The SAXS curves from the QNPHOS-PEO/PMAA solutions were fitted to the Pedersen-Gerstenberg (PG) form factor of the hard sphere with the scattering length  $\rho_s N_{\text{agg}}$  surrounded by  $N_{\text{agg}}$  Gaussian chains with the gyration radius  $r_g$  and excess scattering length  $\rho_c$ . The used model assumes the Schulz-Zimm distribution of the hard sphere radii with the mean radius  $r_0$  and  $k = 1/\sigma^2$ , where  $\sigma$  is the variance:

$$I(q, r_0, k, r_g, \rho_s, \rho_c, N_{\text{agg}}) = \int_0^\infty f(R, r_0, k) P_{\text{mic}}(q, R, R_g, \rho_s, \rho_c, N_{\text{agg}}, d) dR \quad (\text{S4})$$

where the Schulz-Zimm distribution is given by the equation

$$f(R, r_0, k) = \frac{1}{r_0} \left( \frac{R}{r_0} \right)^{k-1} \frac{k^k}{\Gamma(k)} \exp\left( -\frac{kR}{r_0} \right) \quad (\text{S5})$$

and the PG form factor reads

$$P_{\text{mic}}(q, R, r_g, \rho_s, \rho_c, N_{\text{agg}}, d) = N_{\text{agg}}^2 \rho_s^2 F_s(q, R) + N_{\text{agg}} \rho_c^2 F_c(q, r_g) + N_{\text{agg}} (N_{\text{agg}} - 1) \rho_c^2 S_{\text{cc}}(q, R, r_g, d) + 2N_{\text{agg}}^2 \rho_s \rho_c S_{\text{sc}}(q, R, r_g, d) \quad (\text{S6})$$

where the functions  $F_s(q, R)$ ,  $F_c(q, r_g)$ ,  $S_{\text{cc}}(q, R, r_g, d)$  and  $S_{\text{sc}}(q, R, r_g, d)$ , respectively, stand for self-correlation of the sphere, self-correlation of the chains, cross-correlation between the chains and cross-correlation of between the sphere and the chains. They are given by equations

$$F_s(q, R) = 9 \left[ \frac{\sin(qR) - qR \cos(qR)}{(qR)^3} \right]^2 \quad (\text{S7})$$

$$F_c(q, R_g) = 2 \frac{\exp(-r_g^2 q^2) - 1 + r_g^2 q^2}{r_g^4 q^4} \quad (\text{S8})$$

$$S_{\text{cc}}(q, R, R_g, d) = \left[ \frac{1 - \exp(-r_g^2 q^2)}{r_g^2 q^2} \right]^2 \left[ \frac{\sin(qR + qdr_g)}{qR + qdr_g} \right]^2 \quad (\text{S9})$$

$$S_{sc}(q, R, R_g, d) = 3 \left[ \frac{1 - \exp(-r_g^2 q^2)}{r_g^2 q^2} \right] \left[ \frac{\sin(qR) - qR \cos(qR)}{(qR)^3} \right] \left[ \frac{\sin(qR + qdr_g)}{qR + qdr_g} \right] \quad (\text{S10})$$

The parameter  $d$  was set to  $d = 1$  to avoid penetration of the chains into the core region.

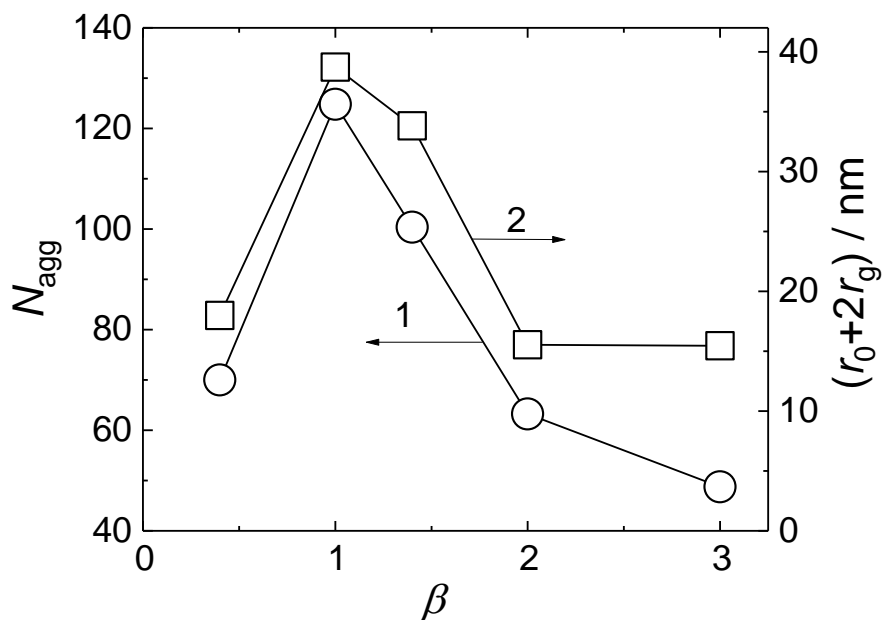


**Fig. S5.**  $N_{agg}$  (curve 1) and the size of the particles,  $r_a + 2r_g$ , (curve 2) obtained from fits of SAXS curves (Fig. 2) by eq. S6 as functions of  $\beta$ .

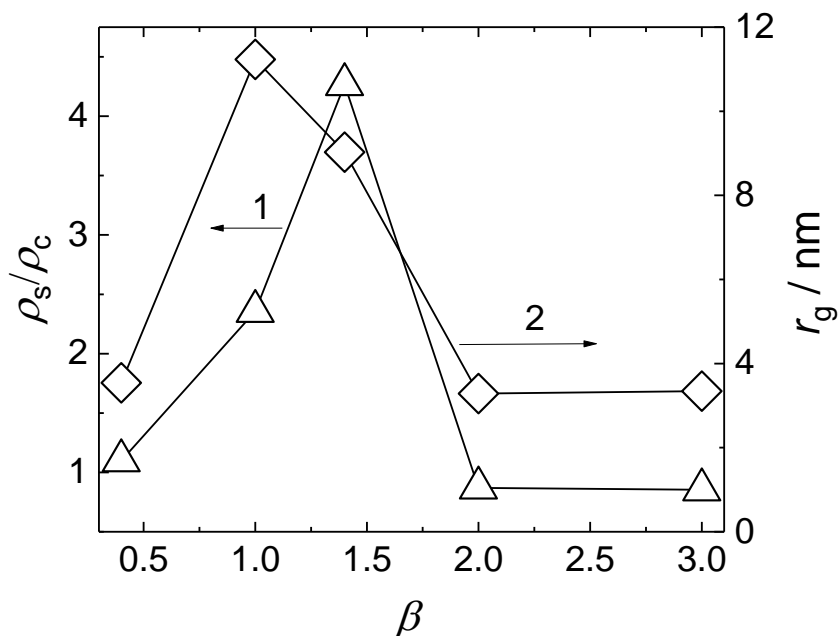


**Fig. S6.**  $\rho_s / \rho_c$  (curve 1) and  $r_g$  (curve 2) obtained from fits of SAXS curves (Fig. 2) by eq. S6 as functions of  $\beta$ .



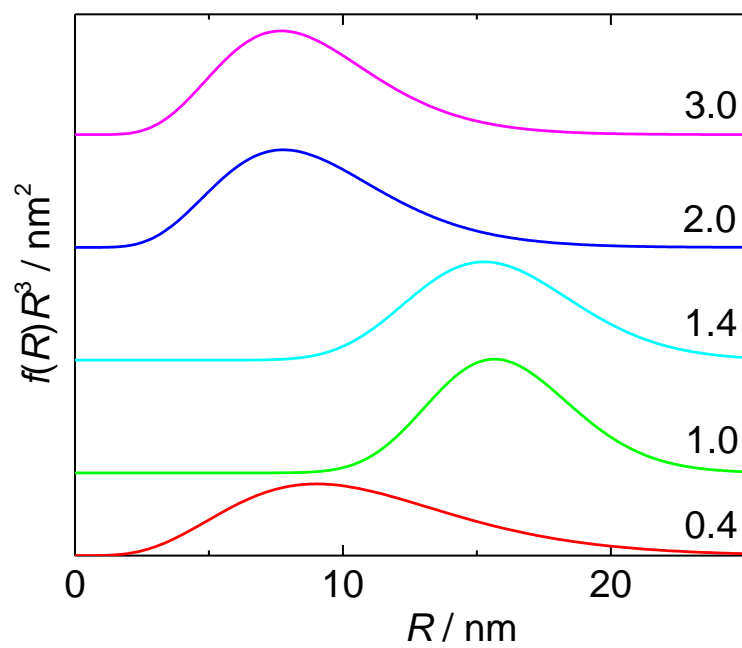


**Fig. S7.** Schulz-Zimm distribution functions for the hard sphere radius, obtained from fits of SAXS curves (Fig. S2) by eq. S6. Molar ratios  $\beta$  are shown above the individual curves.

### 3. AFM scans of QNPHOS-PEO/PMAA aggregates on mica

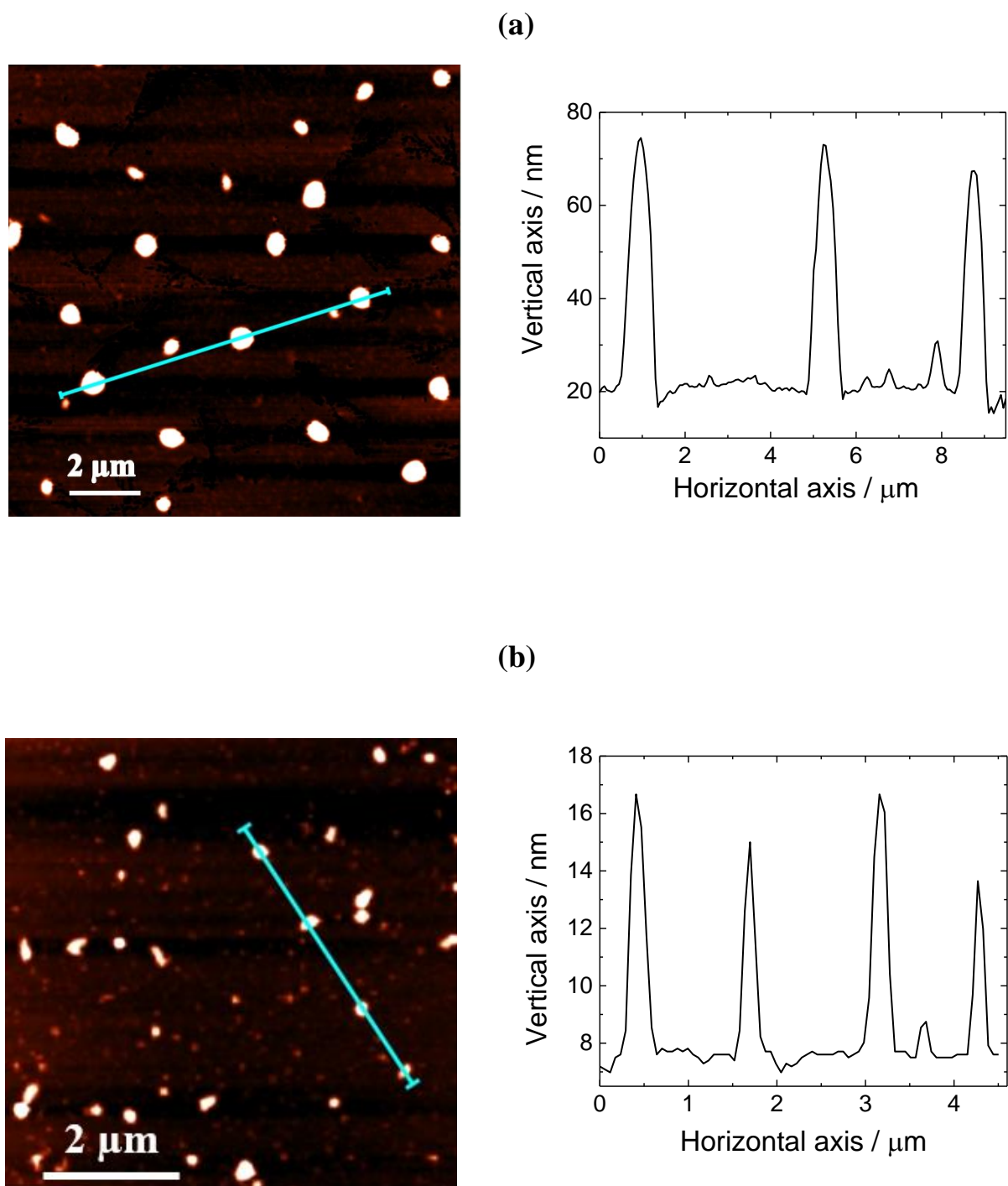


**Fig. S8.** AFM scan and section analysis of QNPHOS-PEO/PMAA aggregates at molar ratios (a)  $\beta=1$  and (b)  $\beta=2$  deposited on mica surface.

#### 4. Thermodynamics and kinetics of PMAA/QNPHOS-PEO complexation from ITC experiments

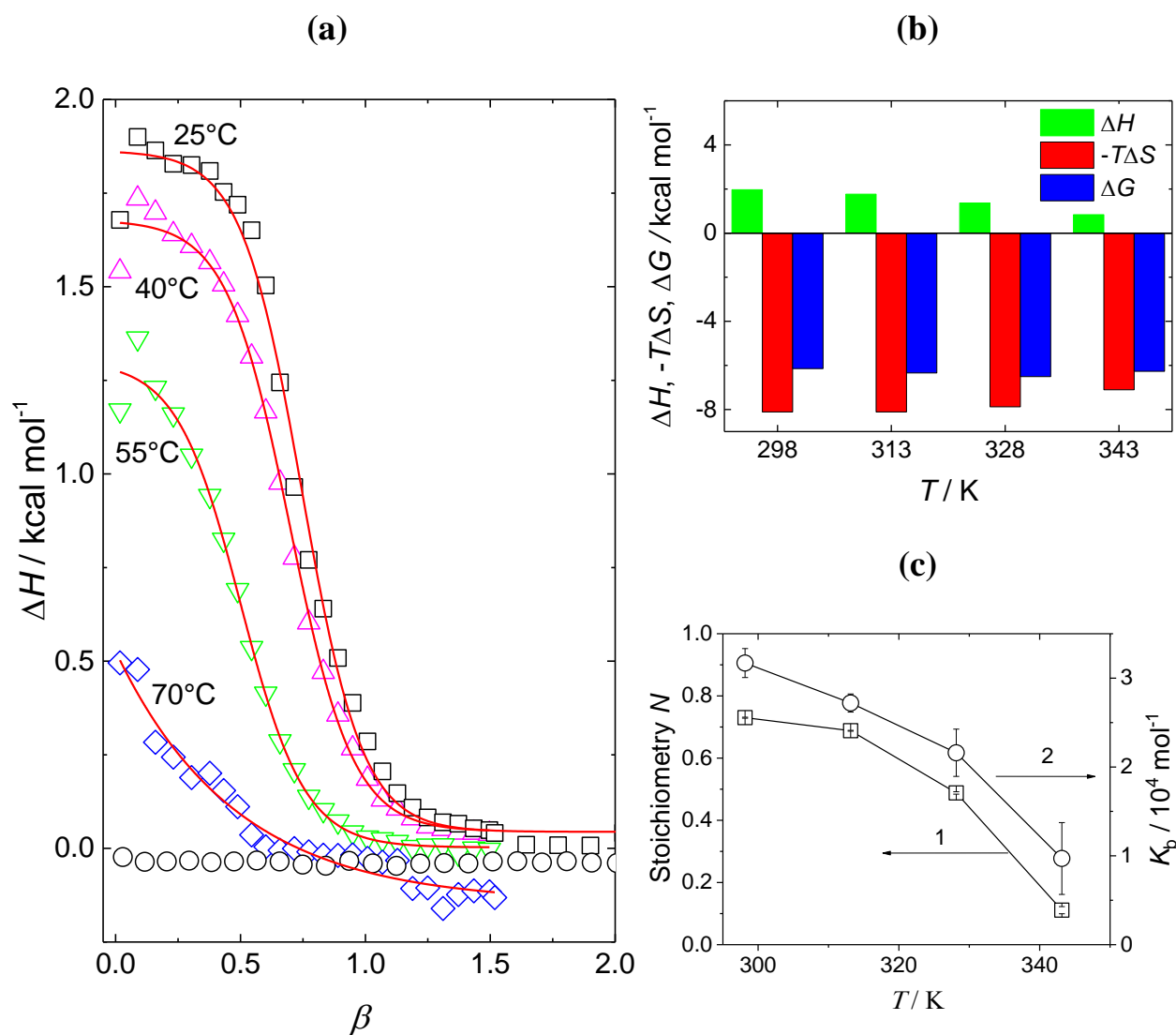
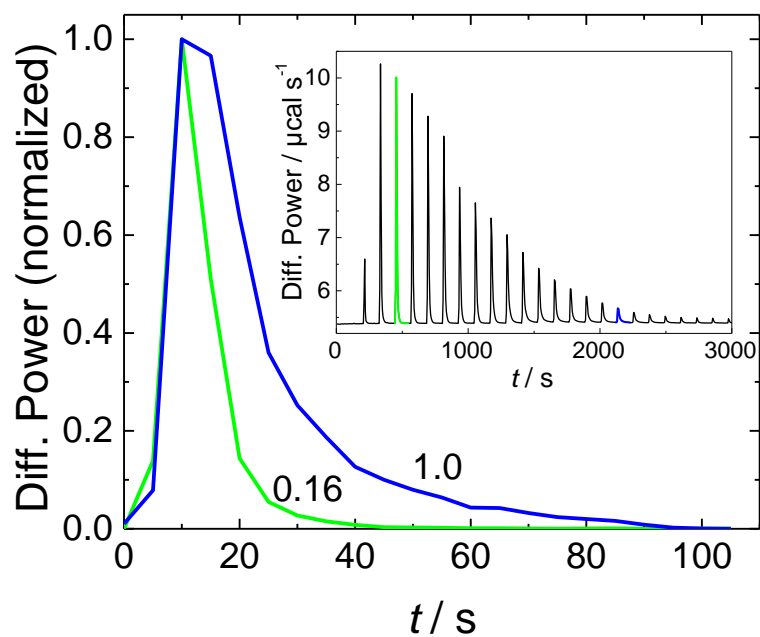


**Fig. S9.** (a) Isothermal calorimetric titration of 1 g L<sup>-1</sup> PMAA solution to 1 g L<sup>-1</sup> QNPHOS-PEO at various temperatures (indicated at individual curves). Red lines are fits of the titration curves with the one-set-of-sites model. Temperature dependence of the thermodynamic parameters: (b) the binding enthalpy,  $\Delta H$ , the binding entropy,  $T\Delta S$ , and the free energy,  $\Delta G$ ; (c) the stoichiometry,  $N$ , (curve 1) and the binding constant,  $K_b$  (curve 2).

(a)



(b)

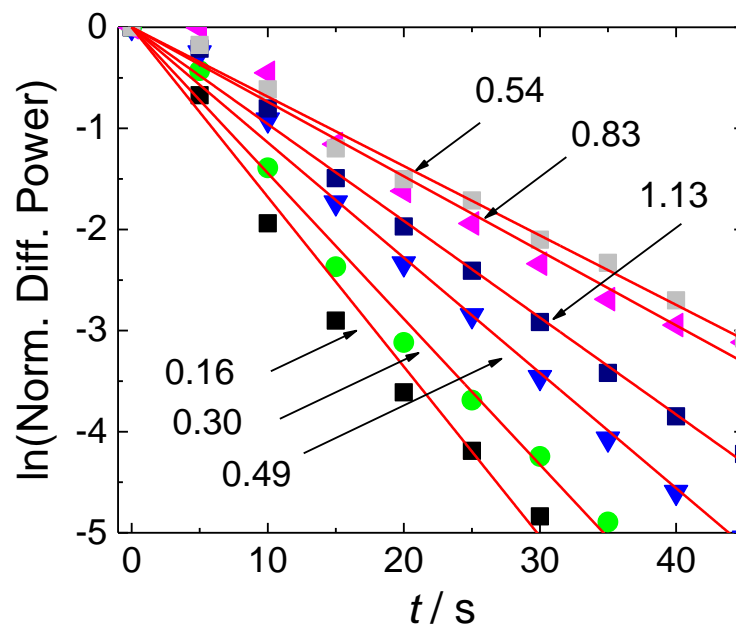


**Fig. S10.** (a) Thermogram for titration of  $1\text{ g L}^{-1}$  PMAA solution to  $1\text{ g L}^{-1}$  QNPHOS-PEO. Insert: normalized ITC differential power for injection number 3 ( $\beta=0.16$ ) and 17 ( $\beta=1.0$ ). (b) Decay of the normalized differential power. The molar ratios,  $\beta$ , of the complexes are indicated above.

## 5. Fluorescence emission spectra and emission decays of umbelliferone in PMAA and QNPHOS-PEO/PMAA solutions

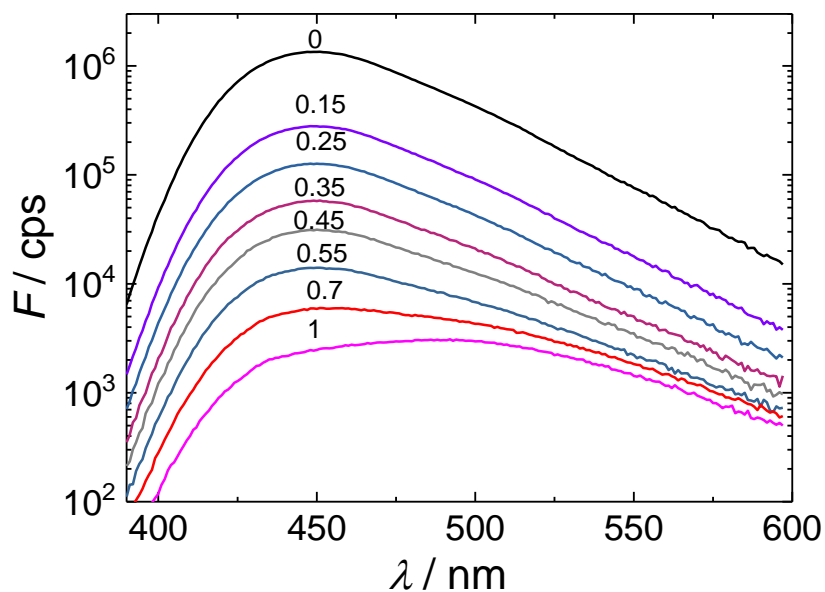


**Fig. S11.** Emission spectra (exc. 378 nm) of umbelliferone label in QNPHOS-PEO/PMAA solutions. Reciprocal molar ratios,  $1/\beta$ , are shown above the individual spectra.

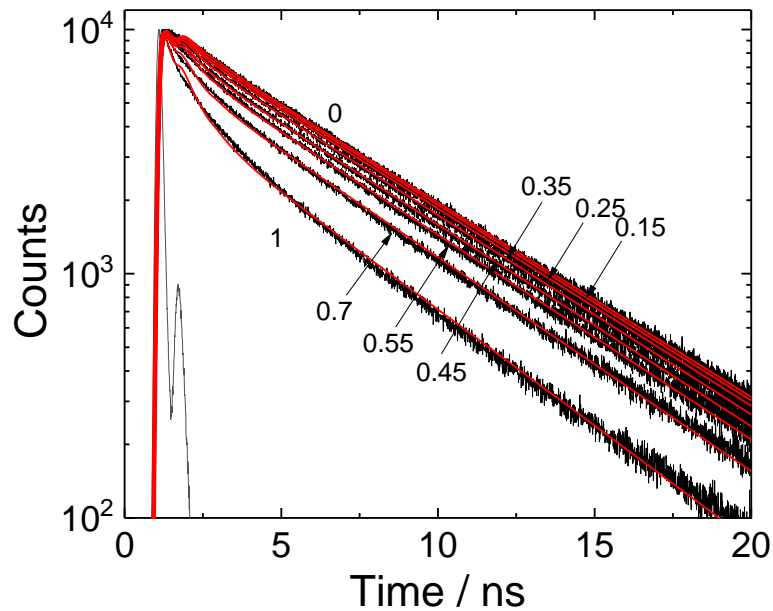


**Fig. S12.** Emission decays at 425 nm (exc. 378 nm) of umbelliferone label in QNPHOS-PEO/PMAA solutions. Reciprocal molar ratios,  $1/\beta$ , are shown above the individual curves. Red curves are fits of the curves to eq. 2.

## 6. Transmittance spectrum of QNPHOS-PEO/PMAA solution

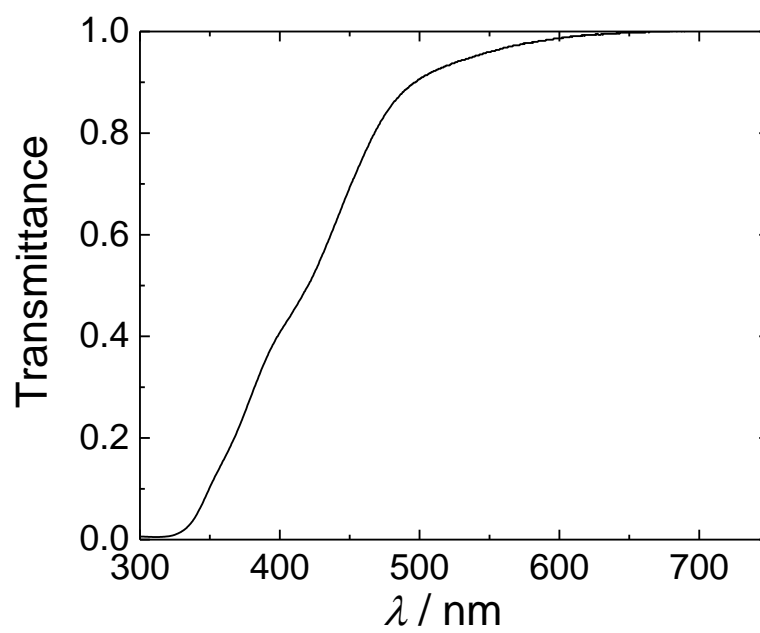


**Fig. S13.** Transmittance spectrum of QNPHOS-PEO/PMAA solution at molar ratio,  $\beta = 1$ .